JACS
JOURNAL OF THE AMERICAN CHEMICAL SOCIETY

Article

General C(sp2)-C(sp3) Cross-Electrophile Coupling Reactions Enabled by Overcharge Protection of Homogeneous Electrocatalysts

Blaise L. Truesdell, Taylor B. Hamby, and Christo S. Sevov

J. Am. Chem. Soc., **Just Accepted Manuscript** • DOI: 10.1021/jacs.0c01475 • Publication Date (Web): 29 Feb 2020

Just Accepted

is published by the American Chemical Society. 1155 Sixteenth Street N.W., Washington, DC 20036

General C(sp^2)-C(sp^3) Cross-Electrophile Coupling Reactions Enabled by Overcharge Protection of Homogeneous Electrocatalysts

Blaise L. Truesdell, Taylor B. Hamby, Christo S. Sevov*

Department of Chemistry and Biochemistry, The Ohio State University, 151 West Woodruff Avenue, Columbus, OH 43210, United States.

Supporting Information Placeholder

ABSTRACT: Cross-electrophile coupling (XEC) of alkyl and aryl halides promoted by electrochemistry represents an attractive alternative to conventional methods that require stoichiometric quantities of high-energy reductants. Most importantly, electroreduction can readily exceed the reducing potentials of chemical reductants to activate catalysts with improved reactivities and selectivities over conventional systems. This work details the mechanistically-driven development of an electrochemical methodology for XEC that utilizes redox-active shuttles developed by the energy-storage community to protect reactive coupling catalysts from overreduction. The resulting electrocatalytic system is practical, scalable, and broadly applicable to the reductive coupling of a wide range of aryl, heteroaryl, or vinyl bromides with primary or secondary alkyl bromides. The impact of overcharge protection as a strategy for electrosynthetic methodologies is underscored by the dramatic differences in yields from coupling reactions with added redox shuttles (generally >80%) and those without (generally <20%). In addition to excellent yields for a wide range of substrates, reactions protected from overreduction can be performed at high currents and on multigram scales.

INTRODUCTION

Metal-catalyzed coupling reactions account for nearly half of all C–C bond-forming reactions that are performed in industry.[1] Classically, cross-product formation relies on the orthogonal reactivities of electrophilic and nucleophilic substrates with the coupling catalyst. Because the nucleophilic substrate is generally an organometallic species that is separately prepared from an electrophile, a more streamlined approach to C–C bond-formation involves the reductive coupling of two electrophilic reagents in a cross-electrophile coupling (XEC).[2] Pioneering work by Périchon,[3–5] Weix[2,6], and Gosmini,[7] along with key advances by Gong,[8–12] Reisman,[13–16] MacMillan,[17] and others,[18–23] has propelled this once-nascent methodology to the forefront of approaches for C–C bond formation.[20,21,24–27]

These reactions are generally catalyzed by Ni complexes, and a metal powder is employed as a chemical reductant. However, these reactions typically require superstoichiometric quantities of the metal powder along with an excesses of a range of other additives and activators.[6,8,17,28] In addition to these concerns for safety and scalability, XEC reactions are most reliable for couplings of primary alkyl halides, while reactions of secondary or tertiary substrates require extensive optimization or a redesign of the catalyst.[8,10,29,30] This limitation is in stark contrast to conventional coupling reactions, which are readily applicable to a wide range of alkyl-magnesium or -zinc reagents and aryl electrophiles.[31–33] A significant advance to the scope of XEC was achieved through the integration of photoredox catalysis as a strategy for activation of substrates.[17] Although these coupling reactions are performed with superstoichiometric quantities of tris(trimethylsilyl)silane as the reductant, their reliability for couplings of a range of substrates has led XEC to be the most common photoredox reaction performed in medicinal chemistry.[24] The industry's dependence on these methodologies underscores the importance of XEC in the synthetic community and highlights the need for scalable and inexpensive strategies for direct coupling of abundant substrates.

Electrochemical reduction in place of chemical reduction or photoredox initiation represents an alternative strategy for XEC reactions because it is inherently applicable to net-reductive processes.[34–37] Electrons can be delivered from benign electron sources at the high energy that is required for reduction. Consequently, energetic chemical reductants, such as metal powders or expensive silanes that preclude large-scale synthesis, can be eliminated from coupling reactions.[17,20] In addition, electrochemistry can readily activate new catalyst systems with improved reactivities and selectivities that require reducing potentials beyond the reductive limits of metal powders. The suitability of electrochemistry as a means to promote XEC is underscored by the fact that the first reports of XEC were performed under electroreductive conditions.[3,38] Recent efforts from both industrial and academic research groups have provided important advances to electrochemical XEC.[39–41] However, these methodologies in their infancy compared to more established strategies for XEC and (*i*) are generally low-yielding with substrates other than primary electrophiles, (*ii*) require divided cells for more complex substrates, (*iii*) are performed at elevated temperatures that often promote protodehalogenation and (*iv*) have low chemical throughput because of low current densities.

In our ongoing effort to develop enabling strategies for electrosynthetic methodologies,[42,43] we report a broadly-applicable, practical, and scalable XEC reaction that can only be performed under electrochemical conditions. A critical component of the methodology is the implementation of a redox shuttle that serves to mitigate overreduction and degradation of the coupling catalyst. This strategy enables electrochemical XEC reactions to be performed with a broad range of secondary alkyl bromides and aryl, heteroaryl, or vinyl bromides. In addition to

high-yielding reactions of these classically-challenging substrates, primary alkyl electrophiles undergo XEC under the developed conditions in near-quantitative yields. This methodology is performed at room temperature and in an undivided cell with inexpensive catalysts and shuttles that are easily prepared on 50 g scales.

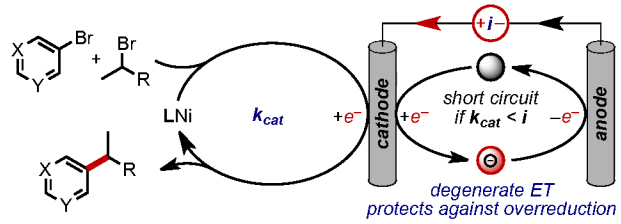

Figure 1. General XEC reactions enabled by the integration of redox co-catalysts for overcharge protection of the coupling catalyst.

Detailed mechanistic studies were key to the development of the electrosynthetic methodology. Electrochemical analyses and stoichiometric reactions of isolated organometallic intermediates implicate overreduction as a key pathway for degradation of the coupling catalyst and formation of undesired organic products. As such, we adapted strategies from the energy storage community on overcharge protection of batteries to mitigate the overreduction of coupling catalysts for XEC. Specifically, electrolysis was performed in the presence of redox-active co-catalysts that serve to shuttle electrons from the cathode to the anode when the rate of reduction exceeds the rate of coupling (Figure 1). This degenerate electron transfer (ET) between electrodes represents a short circuiting of the electrochemical cell and protects the coupling catalyst from further reduction. The dramatic difference in yields from reactions with added redox shuttles (generally >80%) and those without (generally <20%) underscores the remarkable impact of overcharge protection in electrosynthesis. Finally, electrochemical reactions protected from overreduction can be performed at high current densities to form high yields of cross-product in less than 2 h and are readily scaled by two orders of magnitude generate multigram (>17 g) quantities of products with no reduction in yield.

RESULTS AND DISCUSSION

Initial Evaluation of Catalysts for XEC. We first evaluated the reactivities of Ni complexes formed from the pyridyl ligands described in Figure 2 for the electrochemical XEC. Reactions were performed at room temperature and with secondary alkyl electrophiles such that the most reactive and selective coupling catalyst could be identified for this challenging class of alkyl substrates. Electroreduction with a constant current of 3 mA was performed in an undivided cell with a Ni-foam cathode and a Zn anode. Reactions catalyzed by complexes of the tridentate ligands **L1**, **L2**, and **L3** all formed coupled products in low yields along with significant quantities of protodehalogenated byproducts (Figure 2a, entries 1-3). Consistent with previous efforts,[5] complexes of these ligands undergo reduction at mild potentials (>-1.3 V vs. Fc/Fc^+) and form unreactive catalysts for XEC.[30,46,47] Metal complexes of bidentate ligands are generally more reactive toward organic electrophiles than the analogous complexes of tridentate ligands, even if the reduction potentials of the complexes are similar. However, the resulting organonickel complexes of bidentate ligands are generally less stable than the tridentate analogs.[45] As an example, reactions with the Ni complex of bidentate **L4** results in complete conversion of the aryl electrophile but predominantly forms aryl byproducts with only 13% yield of the cross-product (entry 4). We hypothesized that electron-rich tridentate ligands could form catalysts with reactivities that match those of bidentate ligands but would exhibit greater stabilities of the organometallic intermediates. As such, we evaluated reactions catalyzed by Ni-complexes of the x-type, tridentate ligand **L5**. Reduction of the (**L5**)Ni complex requires a more negative potential than any of the other complexes that were evaluated. Because of this low potential, XEC reactions catalyzed by complexes of **L5** that were conducted with chemical reductants failed to generate product and did not even consume the starting materials (see the SI, Figure S2). In contrast, electrochemical reactions catalyzed by same metal-ligand combination formed cross-products in highest yields (43%) and with greatest selectivity over the undesired byproducts (entry 5).

a.

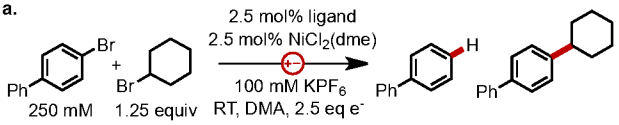

entry	ligand	$E_{1/2}$ (NiL)	%conv	%Ar–H	%Ar–R
1	**L1**	-1.17 V	37	16	20
2	**L2**	-1.27 V	12	4	5
3	**L3**	-1.33 V	36	10	5
4	**L4**	-1.42 V	100	13	13
5	**L5**	-1.72 V	50	7	43

b.

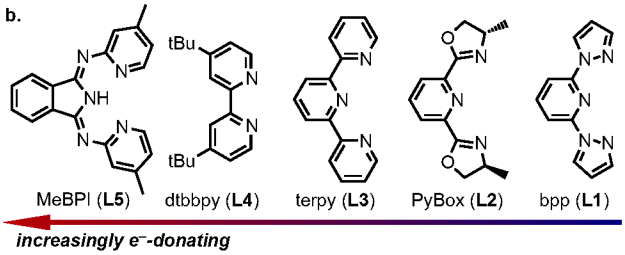

Figure 2. (a) Ligand evaluation for XEC. Reaction products were quantified by calibrated GC analysis against dodecane as an internal standard. (b) Pyridyl-based ligands ordered by electron-releasing properties.

Monitoring the reaction of entry 5, we discovered that most of the coupled product was formed within the first electron equivalent during electrolysis. This finding raised concerns about the stability of the catalyst that operates at such low potentials. Consequently, we monitored the voltaic profiles of the anode and cathode during electrolysis with a pseudo-reference electrode of Ag/Ag^+. Illustrated in Figure 3, the sacrificial Zn anode operates at the expected potential for Zn oxidation (-1 V). Similarly, the initial cathodic voltage of -1.75 V is consistent with reduction of the (**L5**)Ni complex. However, electrolysis at this expected potential is brief (<0.1e^- equivalents), and the cathodic voltage shifts to a more reducing potential of -1.9 V for the remainder of the reaction. We hypothesized that this exceedingly-low voltage could promote the degradation of the coupling catalyst. Given the high reactivity and selectivity at the initial stage of the reaction, we sought to gain further mechanistic insight into this promising electrocatalytic system.

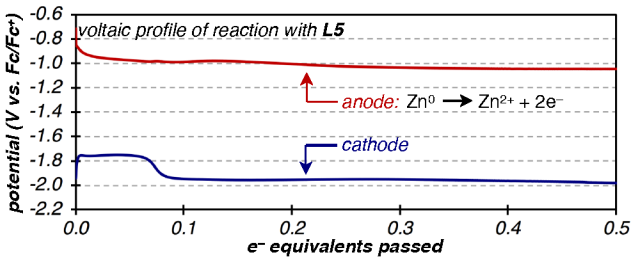

Figure 3. Voltaic profiles of the Zn anode (red) and Ni-foam cathode (blue) from standard reactions catalyzed by complexes of **L5**.

Studies on Catalyst Reactivity and Degradation. We first prepared the **L5**-ligated Ni complex (**1**) according to the synthetic route illustrated in Figure 4. This complex is easily synthesized on >50 g scales by ligation of the isolated **L5** or by templated synthesis of the ligand around $Ni(OAc)_2$.[48] Cyclic voltammetry (CV) of **1** in electrolytes that mimic the reaction conditions reveals two reversible couples at -1.72 V and -1.96 V vs. Fc/Fc^+ (Figure 4, black trace). While this second couple (-1.96 V) is similar to the cathodic potential that was observed during electrolysis, we discovered that complex **1** is rapidly converted into the Ni(aryl) complex **2** when CVs are performed in the presence of phenyl bromide (blue trace). The complex **2** was independently synthesized by transmetalation of diphenyl zinc with **1**, and CV analysis (red trace) of this isolated complex matches the species that is formed during CV analysis of solutions containing both **1** and phenyl bromide (blue trace). This rapid electro-induced activation of an aryl bromide by complex **1** is in stark contrast to the inactivity of other Ni complexes of tridentate ligands (see the Supporting Information, Figure S5). The rapid conversion of complex **1** to **2** in the presence of an aryl bromide indicates that reduction through the second couple of **1** (-1.96 V) is not the origin of the observed potential during catalytic reactions.

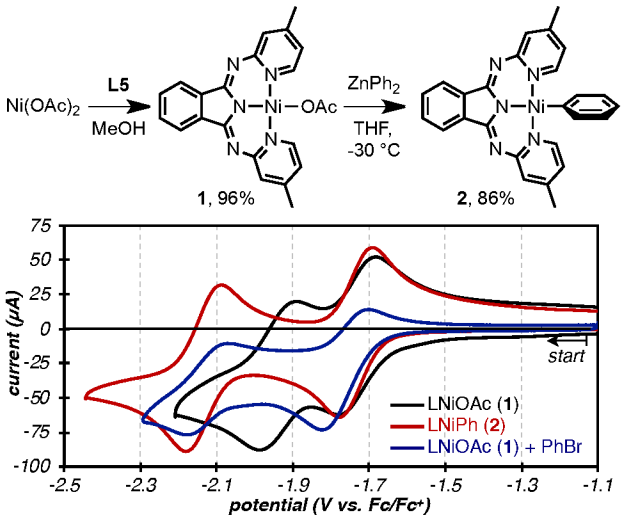

Figure 4. Synthesis and CVs of Ni complexes **1** and **2**. Conditions: 5 mM in DMF with 0.25 M $TBAPF_6$ as electrolyte and a 100 mV/s scan rate using a glass carbon WE and Pt CE. Potentials were calibrated with Fc as an internal standard.

We next investigated the reactivity of complex **2**. Electrolysis of stoichiometric quantities of Ni(aryl) **2** in the presence of cyclohexylbromide formed the coupled product in 95% yield. These results confirm that **2** is an on-cycle intermediate to cross-coupling. However, electrolysis still occurred at a potential that falls between the two couples of complex **2**. Because overpotentials in the cell can shift the potential at which electrolysis occurs from a measured redox potential, we sought to chemically synthesize the reduced forms of the Ni(aryl) complex **2** and evaluate their reactivities. Illustrated in Figure 5a, the singly-reduced form of **2** can be prepared as the sodium salt following chemical reduction with sodium anthracenylide. Electron paramagnetic resonance (EPR) spectroscopy of the paramagnetic anion **3** reveals an isotropic resonance with a g-value of 2.014 (see the Supporting Information, Figure S1), which is consistent with localization of the added electron at the ligand.[49,50] CVs of complex **3** reveal redox events at the same potentials as those of its oxidized form (**2**) but occur with a non-zero initial current (Figure 5b, red trace). The positive onset current is consistent with immediate oxidation of **3** at the starting potentials of the CV measurement (-1.1 V).

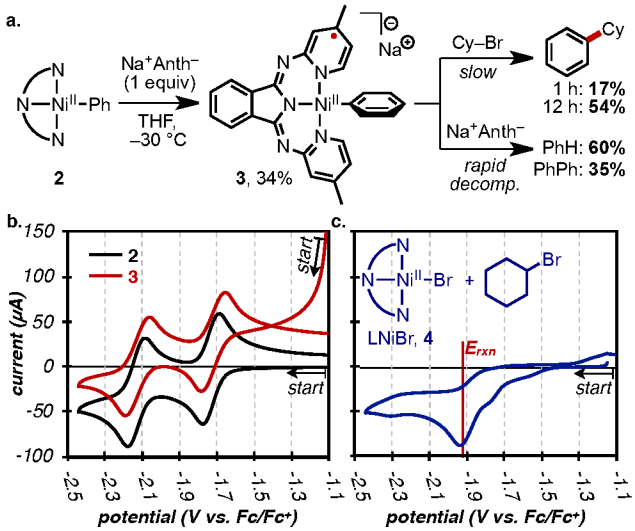

Figure 5. (a) Synthesis and reactivities of reduced forms of complex **2**. (b) CVs of the neutral complex **2** (black trace) and its reduced form (**3**, red trace). (c) CV of isolated LNiBr (**4**) in the presence of alkyl halide and a notation of the observed cathodic potential during catalysis (E_{rxn}). Glassy carbon WE, Pt CE, 0.25 M, DMF, $TBAPF_6$, 100 mV/s scan rate.

The anionic complex **3** is extremely air-sensitive but can be stored in inert atmospheres for weeks and even subjected to elevated temperatures (70 °C) as a solution in DMF without degradation. Addition of an alkyl electrophile to stoichiometric quantities of **3** forms coupled products, but the rate of product formation is much lower than the rate of product formation during electrolysis. Specifically, electrolysis of **2** in the presence of alkyl halide lasts only 30 minutes but forms coupled products in quantitative yields. In contrast, stoichiometric reactions with complex **3** (the chemically-reduced analog of **2**) form coupled products in low yield over the course of 12 hours (Figure 5a). These results indicate that complex **3** is a kinetically incompetent intermediate for the electrochemical reaction. Attempts to further reduce the Ni(aryl) anion (**3**) with a second equivalent of sodium anthracenylide through the redox couple at -2.1 V resulted in rapid degradation of the complex with concomitant formation of the main byproducts encountered in XEC reactions: arene and aryl dimer (Figure 5a).

Results from stoichiometric reactions of complex **2** at various redox states rule out a mechanism of sequential electrophile activation by a reduced Ni(aryl) intermediate.[6,21,27,51–54] We next evaluated the reactivity of the Ni^{II}(bromide) **4**, which can form upon catalyst turnover. Illustrated in Figure 5c, CV of complex **4** in the presence of added alkyl electrophile reveals a reduction event with a catalytic current at the precise potential of the electrochemical reaction. Reduction of analogous nickel halides is known to generate low-valent metal centers that mediate rapid halogen abstraction from alkyl halides to form carbon-centered radicals.[53,55–63] The resulting radical is likely captured by the Ni(aryl) complex **2** and subsequently coupled to the aryl fragment.[17,64] Radical clock experiments reveal trapping of the radical to be dependent on the concentration of Ni in solution, which is consistent with a bimetallic mechanism for electrophile activation and coupling (see the SI, Figure S4).[53,61,65] Overall, these data reveal that while a cathodic potential of -1.9 V must be reached for effective XEC coupling, the Ni(aryl) intermediate is susceptible to rapid decomposition from reduction at potentials below -2 V.

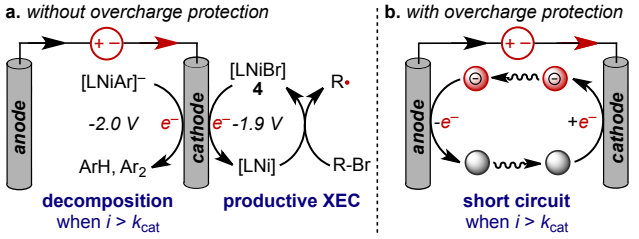

Figure 6. (a) Illustration of productive and destructive processes at the cathode in reactions without shuttles for overcharge protection. (b) Illustration of degenerate shuttling of electrons when the cell voltage approaches the potential of catalyst degradation.

Reaction Development. Guided by these mechanistic insights, we hypothesized that catalyst degradation occurs because the required voltage to initiate XEC (-1.9 V) is within only 100 mV of the onset potential for overreduction of the Ni(aryl) intermediate **2**. Illustrated in Figure 6a, competitive overreduction at -2 V could easily occur as a kinetic reduction, given the small difference in potentials, or could occur in reactions with slow mass transport or catalyst turnover. As a result, electrochemical reactions with catalytic quantities of complex **1** are low yielding, while electrolysis with stoichiometric quantities of **1** reveal the complex to be highly reactive and selective for XEC. To mitigate catalyst overreduction and degradation, we sought to adapt strategies from the battery community that were developed specifically for overcharge protection to XEC reactions.[66–73]

Despite the disparity in research areas, the energy-storage community has encountered and resolved issues of overreduction or overoxidation that closely parallel the identified causes of catalyst degradation in the targeted methodology.[73,74] Like in the XEC reactions, a constant current is employed to charge batteries to a preset capacity. However, electrode degradation over time limits the charging capacity of the battery. As a result, aged batteries are susceptible to dangerous overcharging beyond the capacities of the storage materials. As a means to protect the cathode from overoxidation, homogeneous redox shuttles are added to electrolyte solutions of solid-state batteries. These shuttles are often based on organic compounds with redox potentials that are *greater* than the voltage needed to oxidize (charge) the cathode. This design element allows the cathode to charge without interference from the shuttle. Once the cathode has reached its limited capacity, the oxidizing potential will increase to maintain the constant current. It is once this high voltage is reached that oxidation of the shuttle commences, thereby sparing the cathode of further oxidation. The solvated shuttle can then diffuse to the anode and undergo reduction to short-circuit the overcharging battery and regenerate the overcharge protector (Figure 6). *Thus, an overcharge protector is a catalyst for shuttling electrons that is triggered only when electrolysis exceeds the capacity of the system.*

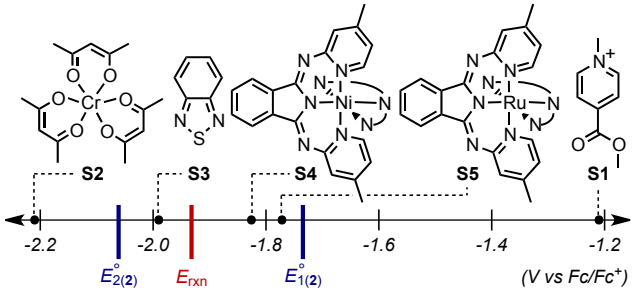

Figure 7. Redox potentials of the evaluated shuttles and of the coupling catalyst **2**.

The conceptual similarities between battery design and the encountered challenges for electroreductive XEC led us to evaluate overcharge protection as a strategy that could sustain catalyst activity when the applied current exceeds the rate of catalytic turnover or mass transport. Plotted in Figure 7 are the standard potentials of shuttle candidates that have been employed in non-aqueous flow batteries because of their reversible redox chemistry and high persistence in all redox states (**S1**-**S5**).[75–79] These shuttles were deliberately selected because their potentials bracket the key redox events of the coupling catalyst **2** (Figure 7, red and blue markers).

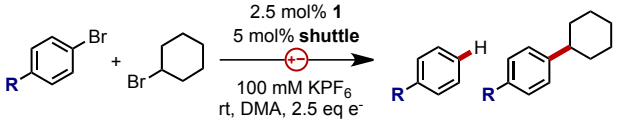

entry	shuttle ($E_{1/2}$)	R group	%Ar–H	%Ar–Cy
1	None	–Ph	7	43
2	None	–CO_2Et	5	5
3	**S1** (-1.21 V)	–Ph	11	9
4	**S2** (-2.21 V)	–Ph	18	22
5	**S3** (-1.99 V)	–Ph	68	4
6	**S4** (-1.82 V)	–Ph	3	97
7	**S4** (-1.82 V)	–CO_2Et	9	89
8	**S5** (-1.78 V)	–Ph	13	71
9	7.5 mol% **1** only	–Ph	18	74
10	7.5 mol% **S4** only	–Ph	11	16

Figure 8. Evaluation of the effect of redox shuttles on the XEC reaction. $E_{1/2}$ values were measured against an internal standard of Fc. Reaction products were quantified by calibrated GC analysis against dodecane as an internal standard.

The electrochemical XEC reactions catalyzed by complex **1** were evaluated with co-catalytic quantities of added redox shuttles for the coupling of bromobiphenyl or bromobenzoate (Figure 8). Coupling of the benzoate electrophile was particularly ineffective under the conditions with just **1** as catalyst (5% yield, entry 2). Reactions performed with 5 mol% of the high-

potential pyridinium shuttle (**S1**) significantly decreased the yield of coupled product compared to the standard reaction (entry 3 vs 1) These reactions operate at low cell voltages (<0.2 V), which suggests that **S1** precludes reduction of the bond-forming catalyst entirely. Shuttles with more negative potentials than the coupling reaction (**S2**) failed to mitigate protodehalogenation (entry 4). Similarly, reactions with just 5 mol% of benzothiadiazole **S3** failed to yield cross products but proceeded with high conversion and almost complete selectivity for protodehalogenation (entry 5). This shuttle (**S3**) has a redox event that falls between the observed potential of electrolysis (-1.9 V) and the unstable redox couple of **2** (-2.1 V). These insights led us to evaluate shuttles with potentials that are more positive than that which is required for electrolysis (>-1.9 V), but more negative than the redox potential of **1** to allow for activation of the aryl bromide (<-1.7 V). The homoleptic complex **S4** with bis(pyridylamino)isoindoline (BPI) ligands is one of the few systems with a reversible redox event (-1.8 V) that falls within this narrow range. Most importantly, reactions performed with co-catalytic quantities of **S4** resulted in dramatically improved yields of coupled products for both bromobiphenyl and bromobenzoate substrates (entries 6 and 7) over the standard reactions. Moreover, these drastic improvements are not limited to reactions with the Ni-based shuttle. A similar increase in the yield of coupled products is observed from reactions with the Ru analog **S5** (entry 8), which falls near the edge of the targeted range. Finally, we performed reactions with high loadings (7.5 mol%) of only **1** or only **S4** to mimic the total loading of redox-active compounds in entries 6 and 7. Reactions with the coupling catalyst or shuttle alone generated products in significantly lower yields of 74% (entry 9) and 16% (entry 10), respectively, compared to 97% from reactions with both **1** and **S4**. In addition to highlighting the synergy between the coupling catalyst and overcharge protector, these data serve as a guide to shuttle selection for future electrocatalytic systems.

Chart 1. Substrate Scope[a]

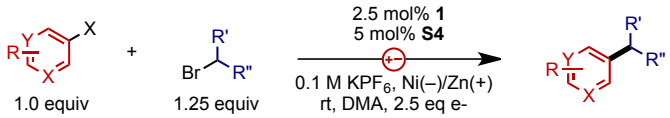

Secondary Alkyl Halides

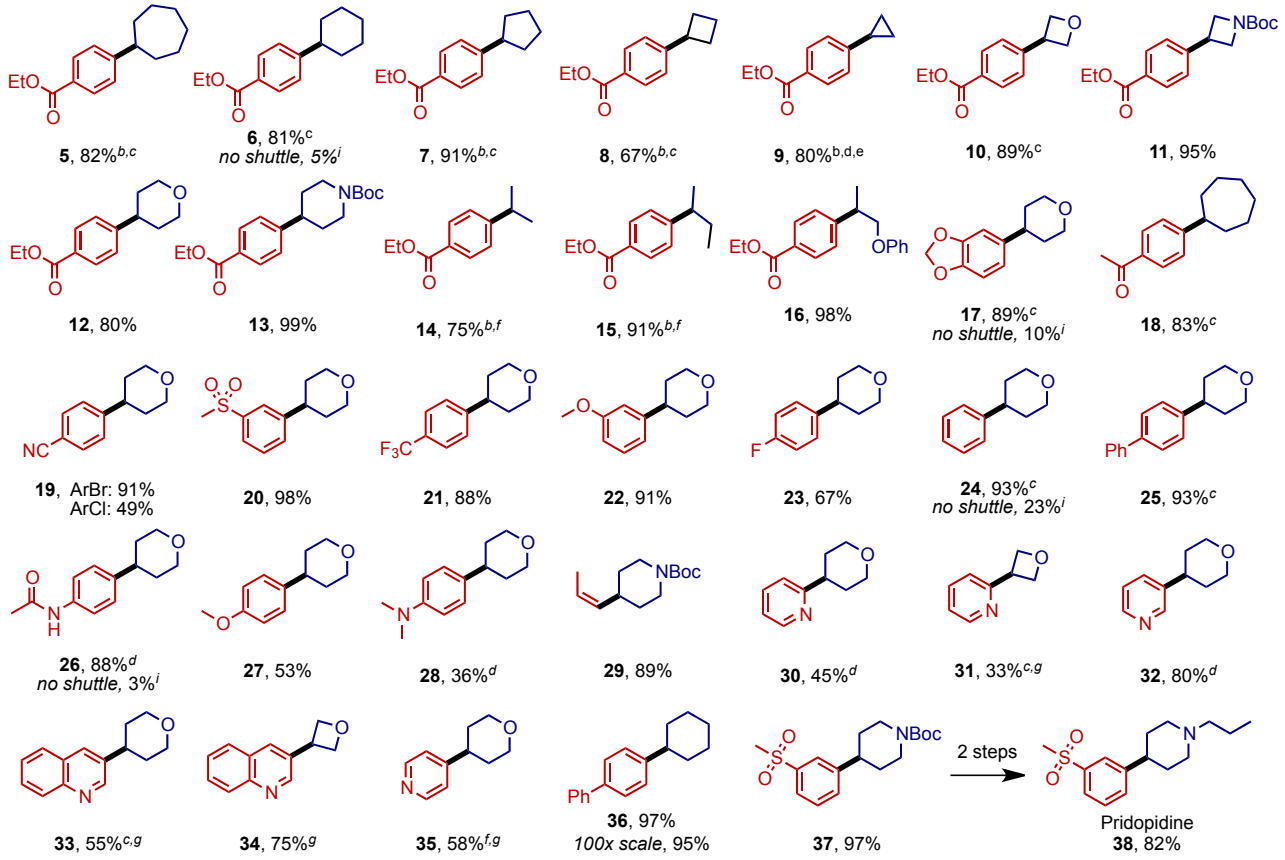

Primary Alkyl Halides

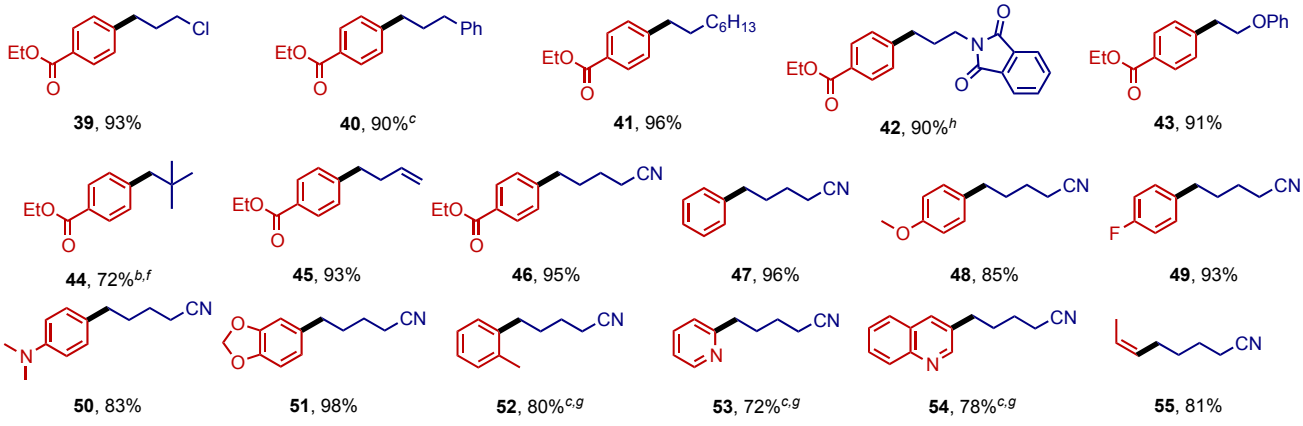

[a]All yields are isolated yields with reaction conditions of aryl halide (0.75 mmol), alkyl halide (1.25 eq), **1** (2.5 mol%), **S4** (5 mol%), KPF_6 (200 mM). [b]2.5 mol% PPh_3 added. [c]1.5 eq alkyl bromide. [d]1.75 eq alkyl bromide. [e]50° C. [f]2 eq alkyl bromide. [g]NaI used in place of KPF_6. [h]No **S4**. [i]GC-FID yields with dodecane as internal standard.

Reaction Scope. With the combination of coupling catalyst and shuttle, we first evaluated the scope of the electrochemical XEC reaction for secondary alkyl electrophiles (Chart 1). Reactions of aryl bromides and alicyclic bromides formed high yields of cross products for all tested ring sizes (entries **5**-**9**).

The high-yielding reaction of cyclopropyl bromide under slightly elevated temperatures (50 °C) is particularly surprising because reductive coupling of this strained electrophile remains rare and is generally low-yielding.[17,28] Similarly, both strained (**10**, **11**) and unstrained (**12**, **13**) heterocyclic alkyl electrophiles were found to be compatible with the XEC reaction, and coupled products were isolated in excellent yields. In addition to alicyclic electrophiles, acyclic alkyl electrophiles undergo coupling without isomerization of the radical intermediate to afford products in high yields (**14**-**16**).

We next evaluated the scope of the aryl halide in coupling reactions with secondary alkyl electrophiles. Despite the reducing conditions, reactions of bromoaryl sulfones or nitriles form cross products in excellent yields without parasitic reduction of the functional groups (**19**, **20**). Such couplings allow Pridopidine (**38**), a late-stage drug candidate,[80] to be rapidly assembled from common electrophiles in high yield (82% overall). Similarly, (*Z*)-vinyl bromides undergo electroreductive coupling without isomerization and form products in excellent yields (89%, **29**) and with complete retention of the (*Z*)-stereochemistry. Haloaryl acetamides or ketones are directly compatible and do not require protection of the respective protic or enolizable groups (**26** and **18**). While electron deficient aryl bromides are generally most reactive, electron-neutral and electron-rich bromoarenes form products in high yields under the mild conditions. However, reactions of substrates with extremely electron-releasing groups, such as *para*-dimethylamino, formed cross products with secondary electrophiles in only modest yields (36%, **28**). Notably, the analogous reaction of a dimethylamino bromobenzene and a *primary* alkyl electrophile forms near-quantitative yields of coupled products (**50**). These latter examples highlight the challenge of coupling secondary alkyl electrophiles compared to primary alkyl electrophiles.

Finally, we investigated reactions of secondary alkyl electrophiles and heteroaryl bromides. Such XEC reactions remain rare,[17,23,81,82] and their electrochemical analogs are unknown. The developed methodology was directly extended to couplings of heteroaryl substrates and generated products in modest to excellent yields. Couplings of 2-bromopyridines and secondary electrophiles proved most challenging, but pyridyl piperidines (**30**) or oxetanes (**31**) were still isolated in 45% and 33% yields, respectively. In contrast, reactions of 3- and 4-bromopyridines or quinolines are generally high-yielding (entries **32**-**35**). In addition to reactions of secondary electrophiles, the electrocatalytic system was successfully applied to the coupling of primary alkyl bromides with a variety of aryl and heteroaryl bromides. In particular, reactions of the most challenging classes of aryl or heteroaryl electrophiles that were identified above, including 2-pyridyl bromides (**53**), *ortho*-substituted bromobenzene (**52**), or *para*-dimethylamino bromobenzene (**50**), all formed products in excellent yields. Finally, we note that reactions do not require rigorously-inert conditions, and mixtures can be prepared outside of a glovebox. Further simplifying the methodology, the target combination of **1** (2.5 mol%) and shuttle **S4** (5 mol%) can be directly generated by prestirring the appropriate ratio of **L5** and $Ni(OAc)_2$ (3:2) at 80 °C in MeOH for 1 h. Upon cooling, an air-stable powder can be isolated by filtration and directly employed as catalyst to form coupled products with no reduction in yield.

Overall, reactions with the developed electrocatalytic system were found to be applicable to a broad range of substrates with high reliability and to be easily scaled (100-fold scale, 75 mmol of **36**). The impact of the developed strategy is underscored by the *extreme* differences in product yields from reactions with added the shuttle and those without. Products **6**, **17**, **24**, and **26** were isolated in a combined average yield of 88% from reactions performed under the standard conditions but are formed with an average yield of only 10% in the absence of the shuttle. *These findings suggest that desirable catalysts – previously evaluated to be ineffective for cross coupling – could exhibit high coupling activity when paired with the appropriate shuttle.*

Role of the Shuttle. The success of the catalyst/shuttle pair inspired us to gain further insight into the role of the shuttle, such that catalyst pairings can be rapidly developed in future methodologies. We first performed catalytic reactions with increasing quantities of the shuttle **S4** and monitored both product formation and consumption of starting materials. As summarized in Figure 9, reactions under the standard conditions of 2.5%-5% **S4** formed products in high yields (blue trace). Omitting the shuttle results in reactions that generate products in low yields yet still consume the majority of the alkyl electrophile (red trace). Reactions with high loadings of **S4** (10%-20%) similarly formed low yields of product but contained significant quantities of unreacted starting materials. Because 2.5 equivalents of electrons were applied to all reactions, these data provide insights into the electron utilization with different shuttle loadings. Specifically, a significant portion of the reducing equivalents are consumed for parasitic degradation of the starting materials in reactions without **S4**. In contrast, a high concentration of the shuttle prevents these reductive degradations but also inhibits product formation. An identical correlation between shuttle loading and conversion is observed for reactions of bromobenzoate (see the SI, Figure S6). We hypothesize that electrons are preferentially shuttled back to the anode rather than utilized for coupling in reactions with high concentrations of **S4**. These degenerate redox events (reduction of **S4** at the cathode and oxidation of $\mathbf{S4}^-$ at the anode) are a low-voltage alternative to cross coupling and represent a short circuit. An accounting of the electrons that were utilized for coupling provides further evidence that high loadings of **S4** promote unproductive ET. Specifically, the total quantity of converted reactants and formed products in reactions with high loadings of **S4** accounts for only 52% of the applied electrons during electroreduction. The remaining 48% of the passed electrons remain unaccounted for and were likely consumed by degenerate electron shuttling, rather than bonding-forming processes.

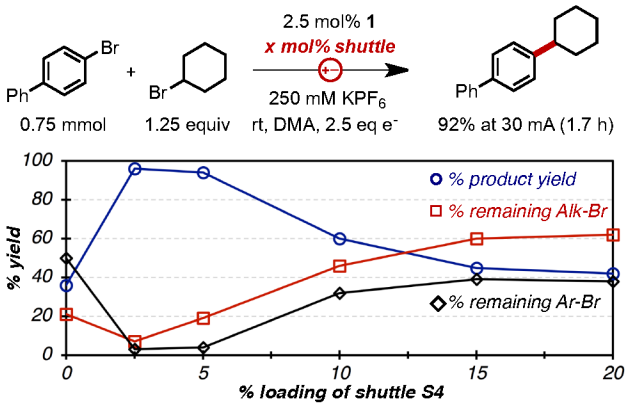

Figure 9. Effect of the shuttle loading on the formation of product (blue trace) and consumption of alkyl and aryl bromides (red and black traces).

These insights suggest that the shuttle serves as an internal limiter that is enabled when the rate of electrolysis (current) exceeds the rate of catalysis. This concept led us to evaluate reactions at high currents that would be limited only by the turnover frequency of the coupling catalyst. High current densities are particularly important for chemical throughput, but electroreductive reactions are generally performed at low current densities (<0.5 mA/cm^2).[40,83] Similarly, highest yields are obtained at low currents with the standard loadings of shuttle. However reactions conducted with slightly increased loadings of **S4** (10 mol%) and Ni-cathodes of just 1 cm x 1 cm submerged in solution can be performed at currents up to 30 mA to generate coupled products in high yields (92%) in under 2 h.[84] The impact of the high current densities on product throughput was highlighted by a reaction that was performed on a 75 mmol scale (>17 g) at 400 mA to form the cross-product **36** in 85% yield after just 12 h. The slight decrease in yield is likely the result of elevated temperatures (35-40 °C) that result from the increased resistance due to the large electrode separation and high current density at the Zn plate. We anticipate that even greater throughput with no loss in yield can be achieved with improved engineering of the reactors or by performing the reactions in flow.

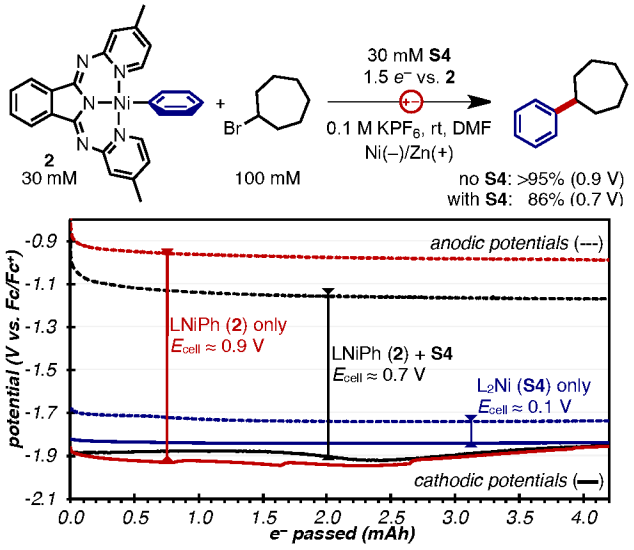

Figure 10. Comparison of operating potentials of the anodes (dashed lines) and cathodes (solid line) from the stoichiometric reactions illustrated above.

Finally, we sought to gain further insight into the redox events at the anode and cathode under the developed conditions. Degenerate ET by the shuttle would result in anodic and cathodic voltages that are both at the standard potential of **S4** ($E_{1/2}$ = -1.82 V) and a net cell voltage of zero. Electrolysis under the catalytic conditions with a pseudo-reference electrode failed to reveal significant changes to the anodic or cathodic potentials when reactions were performed with or without **S4**. We attribute these results to the low concentrations of shuttle in solution, such that Zn oxidation is the predominant reaction at the anode compared to the occasional oxidation of **S4**$^-$. Consequently, we performed studies with high concentrations of shuttle and stoichiometric quantities of the isolated Ni(aryl) intermediate **2** in the presence of excess alkyl electrophile. Illustrated in Figure 10 (red trace), electrolysis of **2** in the absence of added shuttle formed coupled product in quantitative yield and occurred with an E_{cell} of 0.9 V. The pseudo-reference electrode reveals that the measured cell voltage results from oxidation at -1 V (vs Fc/Fc$^+$) and reduction at -1.9 V. Electrolysis performed with added **S4** had no change in the operating potential of the cathode, but shifted the potential of the anode to a more negative voltage (-1.1 V, black trace). Because **S4** has no redox event at -1.1 V, the negative shift in anodic potential is likely the result of competitive oxidation of the reduced shuttle at -1.8 V in preference to Zn (-1 V). Additionally, the yield of coupled product is only 85%, and quantitative yields required an additional 0.5 equivalents of e-. These results indicate that a significant portion of the reducing equivalents were consumed through degenerate shuttling rather than coupling. A more drastic shift in anodic potential was observed when electrolysis was performed with only the shuttle in solution (blue trace). With no possibility for cross coupling, the anode and cathode operate at nearly identical potentials of -1.8 V. The resulting E_{cell} of just 0.1 V is consistent with a degenerate transfer of electrons by the shuttle.

CONCLUSION

In summary, this work details the strategic integration of redox-active molecules developed by the energy-storage community into electrochemical XEC reactions to protect desirable coupling catalysts from overreduction. The resulting electrocatalytic system is practical, scalable, and broadly applicable to the reductive coupling of a wide range of aryl, heteroaryl, or vinyl bromides with primary or secondary alkyl bromides. The dramatic influence of overcharge protection on coupling reactions is particularly striking in outcomes of reactions of secondary alkyl electrophiles, which are generally lower-yielding and less reliable than reactions of primary alkyl electrophiles. Specifically, isolated yields of such reactions with overcharge protection generally exceed 80%, while unprotected reactions form coupled products in less than 20% yield.

The generality of this coupling system rivals or exceeds the current state-of-the-art for XEC reactions that often require superstoichiometric additives, expensive reductants, or specially-designed ligands. In contrast, the developed reactions are performed (*i*) with inexpensive catalysts and shuttles that are accessible in a single step on >50 g scales, (*ii*) at ambient temperatures with a strip of Zn, and (*iii*) at high currents on large scales. Detailed mechanistic studies of isolated organometallic complexes in their various redox states were critical in identifying decomposition pathways and developing catalyst-shuttle pairs. To the best of our knowledge, this report represents the first example that explicitly details overcharge protection as a strategy for improving electrocatalytic methodologies. However, we anticipate that overcharge protection could be a general strategy for the protection of desirable electrocatalysts from overreduction or overoxidation and applicable to a wide range of electrochemically-induced catalytic reactions.

ASSOCIATED CONTENT

Supporting Information

Experimental procedures, cell design, characterization of compounds, spectroscopic data, x-ray data, electrochemical data, and additional experiments are supplied. This material is available free of charge via the Internet at http://pubs.acs.org.

AUTHOR INFORMATION

Corresponding Author

sevov.1@osu.edu

ACKNOWLEDGMENT

We thank The Ohio State University and the American Chemical Society Petroleum Research Fund for support of this work.

REFERENCES

(1) Roughley, S. D.; Jordan, A. M. The Medicinal Chemist's Toolbox : An Analysis of Reactions Used in the Pursuit of Novel Drug Candidates. *J. Med. Chem.* **2011**, *54* (10), 3451–3479. https://doi.org/10.1021/jm200187y.

(2) Everson, D. A.; Shrestha, R.; Weix, D. J. Nickel-Catalyzed Reductive Cross-Coupling of Aryl Halides with Alkyl Halides. *J. Am. Chem. Soc.* **2010**, *132* (3), 920–921. https://doi.org/10.1021/ja9093956.

(3) Durandetti, M.; Nédélec, J. Y.; Périchon, J. Nickel-Catalyzed Direct Electrochemical Cross-Coupling between Aryl Halides and Activated Alkyl Halides. *J. Org. Chem.* **1996**, *61* (5), 1748–1755. https://doi.org/10.1021/jo9518314.

(4) Durandetti, M.; Périchon, J. Nickel-Catalyzed Electrochemical Coupling of Aryl, Heteroaryl or Vinyl Halides with Activated Alkyl Chlorides: Synthetic and Stereochemical Aspects. *Synthesis (Stuttg).* **2004**, No. 18, 3079–3083. https://doi.org/10.1055/s-2004-834896.

(5) Nédélec, J.-Y.; Périchon, J.; Troupel, M. Organic Electroreductive Coupling Reactions Using Transition Metal Complexes as Catalysts. In *Electrochemistry VI Electroorganic Synthesis: Bond Formation at Anode and Cathode*; Steckhan, E., Ed.; Springer Berlin Heidelberg: Berlin, Heidelberg, 1997; pp 141–173. https://doi.org/10.1007/3-540-61454-0_72.

(6) Weix, D. J. Methods and Mechanisms for Cross-Electrophile Coupling of Csp^2 Halides with Alkyl Electrophiles. *Acc. Chem. Res.* **2015**, *48* (6), 1767–1775. https://doi.org/10.1021/acs.accounts.5b00057.

(7) Amatore, M.; Gosmini, C. Direct Method for Carbon-Carbon Bond Formation: The Functional Group Tolerant Cobalt-Catalyzed Alkylation of Aryl Halides. *Chem. - A Eur. J.* **2010**, *16* (20), 5848–5852. https://doi.org/10.1002/chem.201000178.

(8) Gu, J.; Qiu, C.; Lu, W.; Qian, Q.; Lin, K.; Gong, H. Nickel-Catalyzed Reductive Cross-Coupling of Vinyl Bromides with Unactivated- Alkyl Halides. *Synthesis (Stuttg).* **2017**, *49* (08), 1867–1873. https://doi.org/10.1055/s-0036-1588132.

(9) Liu, J.; Gong, H. Stereoselective Preparation of α-C-Vinyl/Aryl Glycosides via Nickel-Catalyzed Reductive Coupling of Glycosyl Halides with Vinyl and Aryl Halides. *Org. Lett.* **2018**, *20* (24), 7991–7995. https://doi.org/10.1021/acs.orglett.8b03567.

(10) Wang, X.; Wang, S.; Xue, W.; Gong, H. Nickel-Catalyzed Reductive Coupling of Aryl Bromides with Tertiary Alkyl Halides. *J. Am. Chem. Soc.* **2015**, *137* (36), 11562–11565. https://doi.org/10.1021/jacs.5b06255.

(11) Xu, H.; Zhao, C.; Qian, Q.; Deng, W.; Gong, H. Nickel-Catalyzed Cross-Coupling of Unactivated Alkyl Halides Using Bis(Pinacolato)Diboron as Reductant. *Chem. Sci.* **2013**, *4* (10), 4022–4029. https://doi.org/10.1039/C3SC51098K.

(12) Wang, X.; Dai, Y.; Gong, H. Nickel-Catalyzed Reductive Couplings. *Top. Curr. Chem.* **2016**, *374* (4), 43. https://doi.org/10.1007/s41061-016-0042-2.

(13) Cherney, A. H.; Reisman, S. E. Nickel-Catalyzed Asymmetric Reductive Cross-Coupling between Vinyl and Benzyl Electrophiles. *J. Am. Chem. Soc.* **2014**, *136* (41), 14365–14368. https://doi.org/10.1021/ja508067c.

(14) Kadunce, N. T.; Reisman, S. E. Nickel-Catalyzed Asymmetric Reductive Cross-Coupling between Heteroaryl Iodides and α-Chloronitriles. *J. Am. Chem. Soc.* **2015**, *137* (33), 10480–10483. https://doi.org/10.1021/jacs.5b06466.

(15) Cherney, A. H.; Kadunce, N. T.; Reisman, S. E. Enantioselective and Enantiospecific Transition-Metal-Catalyzed Cross-Coupling Reactions of Organometallic Reagents to Construct C-C Bonds. *Chem. Rev.* **2015**, *115* (17), 9587–9652. https://doi.org/10.1021/acs.chemrev.5b00162.

(16) Suzuki, N.; Hofstra, J. L.; Poremba, K. E.; Reisman, S. E. Nickel-Catalyzed Enantioselective Cross-Coupling of N-Hydroxyphthalimide Esters with Vinyl Bromides. *Org. Lett.* **2017**, *19* (8), 2150–2153. https://doi.org/10.1021/acs.orglett.7b00793.

(17) Zhang, P.; Le, C. "Chip" C.; MacMillan, D. W. C. Silyl Radical Activation of Alkyl Halides in Metallaphotoredox Catalysis: A Unique Pathway for Cross-Electrophile Coupling. *J. Am. Chem. Soc.* **2016**, *138* (26), 8084–8087. https://doi.org/10.1021/jacs.6b04818.

(18) Konev, M. O.; Hanna, L. E.; Jarvo, E. R. Intra- and Intermolecular Nickel-Catalyzed Reductive Cross-Electrophile Coupling Reactions of Benzylic Esters with Aryl Halides. *Angew. Chemie - Int. Ed.* **2016**, *55* (23), 6730–6733. https://doi.org/10.1002/anie.201601206.

(19) Erickson, L. W.; Lucas, E. L.; Tollefson, E. J.; Jarvo, E. R. Nickel-Catalyzed Cross-Electrophile Coupling of Alkyl Fluorides: Stereospecific Synthesis of Vinylcyclopropanes. *J. Am. Chem. Soc.* **2016**, *138* (42), 14006–14011. https://doi.org/10.1021/jacs.6b07567.

(20) Knappke, C. E. I.; Grupe, S.; Gärtner, D.; Corpet, M.; Gosmini, C.; Jacobi Von Wangelin, A. Reductive Cross-Coupling Reactions between Two Electrophiles. *Chem. - A Eur. J.* **2014**, *20* (23), 6828–6842. https://doi.org/10.1002/chem.201402302.

(21) Lucas, E. L.; Jarvo, E. R. Stereospecific and Stereoconvergent Cross-Couplings between Alkyl Electrophiles. *Nat. Rev. Chem.* **2017**, *1* (9), 0065. https://doi.org/10.1038/s41570-017-0065.

(22) Gadde, S. K.; Peshkov, A.; Brzozowska, A.; Nikolaienko, P.; Zhu, C.; Rueping, M. Nickel Catalyzed Chain Walking Cross-Electrophile Coupling of Alkyl and Aryl Halides and Olefin Hydroarylation Enabled by Electrochemical Reduction. *Angew. Chemie Int. Ed.* **2020**, n/a, n/a. https://doi.org/10.1002/anie.201915418.

(23) Molander, G. A.; Traister, K. M.; ONeill, B. T. Reductive Cross-Coupling of Nonaromatic, Heterocyclic Bromides with Aryl and Heteroaryl Bromides. *J. Org. Chem.* **2014**, *79* (12), 5771–5780. https://doi.org/10.1021/jo500905m.

(24) Le, C. "Chip" C.; Wismer, M. K.; Shi, Z.-C. C.; Zhang, R.; Conway, D. V.; Li, G.; Vachal, P.; Davies, I. W.; MacMillan, D. W. C. A General Small-Scale Reactor To Enable Standardization and Acceleration of Photocatalytic Reactions. *ACS Cent. Sci.* **2017**, *3* (6), 647–653. https://doi.org/10.1021/acscentsci.7b00159.

(25) Richmond, E.; Moran, J. Recent Advances in Nickel Catalysis Enabled by Stoichiometric Metallic Reducing Agents. *Synth.* **2018**, *50* (3), 499–513. https://doi.org/10.1055/s-0036-1591853.

(26) Li, Y.; Fan, Y.; Jia, Q. Recent Advance in Ni-Catalyzed Reductive Cross-Coupling to Construct $C(sp^2)$-$C(sp^2)$ and $C(sp^2)$-$C(sp^3)$ Bonds . *Chinese J. Org. Chem.* **2019**, *39* (2), 350. https://doi.org/10.6023/cjoc201806038.

(27) Everson, D. A.; Weix, D. J. Cross-Electrophile Coupling: Principles of Reactivity and Selectivity. *J. Org. Chem.* **2014**, *79* (11), 4793–4798. https://doi.org/10.1021/jo500507s.

(28) Yu, X.; Yang, T.; Wang, S.; Xu, H.; Gong, H. Nickel-Catalyzed Reductive Cross-Coupling of Unactivated Alkyl Halides. *Org. Lett.* **2011**, *13* (8), 2138–2141. https://doi.org/10.1021/ol200617f.

(29) Wang, X.; Ma, G.; Peng, Y.; Pitsch, C. E.; Moll, B. J.; Ly, T.

D.; Wang, X.; Gong, H. Ni-Catalyzed Reductive Coupling of Electron-Rich Aryl Iodides with Tertiary Alkyl Halides. *J. Am. Chem. Soc.* **2018**, *140*, (43), 14490–14497. https://doi.org/10.1021/jacs.8b09473.

(30) Wang, S.; Qian, Q.; Gong, H. Nickel-Catalyzed Reductive Coupling of Aryl Halides with Secondary Alkyl Bromides and Allylic Acetate. *Org. Lett.* **2012**, *14* (13), 3352–3355. https://doi.org/10.1021/ol3013342.

(31) Lohre, C.; Dröge, T.; Wang, C.; Glorius, F. Nickel-Catalyzed Cross-Coupling of Aryl Bromides with Tertiary Grignard Reagents Utilizing Donor-Functionalized N-Heterocyclic Carbenes (NHCs). *Chem. - A Eur. J.* **2011**, *17* (22), 6052–6055. https://doi.org/10.1002/chem.201100909.

(32) Zultanski, S. L.; Fu, G. C. Nickel-Catalyzed Carbon-Carbon Bond-Forming Reactions of Unactivated Tertiary Alkyl Halides: Suzuki Arylations. *J. Am. Chem. Soc.* **2013**, *135* (2), 624–627. https://doi.org/10.1021/ja311669p.

(33) Joshi-Pangu, A.; Wang, C. Y.; Biscoe, M. R. Nickel-Catalyzed Kumada Cross-Coupling Reactions of Tertiary Alkylmagnesium Halides and Aryl Bromides/Triflates. *J. Am. Chem. Soc.* **2011**, *133* (22), 8478–8481. https://doi.org/10.1021/ja202769t.

(34) Moeller, K. D. Using Physical Organic Chemistry to Shape the Course of Electrochemical Reactions. *Chem. Rev.* **2018**, *118* (9), 4817–4833. https://doi.org/10.1021/acs.chemrev.7b00656.

(35) Horn, E. J.; Rosen, B. R.; Baran, P. S. Synthetic Organic Electrochemistry: An Enabling and Innately Sustainable Method. *ACS Cent. Sci.* **2016**, *2* (5), 302–308. https://doi.org/10.1021/acscentsci.6b00091.

(36) Yan, M.; Kawamata, Y.; Baran, P. S. Synthetic Organic Electrochemical Methods Since 2000: On the Verge of a Renaissance. *Chem. Rev.* **2017**, *117* (21), 13230–13319. https://doi.org/10.1021/acs.chemrev.7b00397.

(37) Ogawa, K. A.; Boydston, A. J. Recent Developments in Organocatalyzed Electroorganic Chemistry. *Chem. Lett.* **2015**, *44* (1), 10–16. https://doi.org/10.1246/cl.140915.

(38) Conan, A.; Sibille, S.; D'Incan, E.; Périchon, J. Nickel-Catalysed Electroreductive Coupling of α-Halogenoesters with Aryl or Vinyl Halides. *J. Chem. Soc. Chem. Commun.* **1990**, No. 1, 48–49. https://doi.org/10.1039/C39900000048.

(39) Perkins, R. J.; Hughes, A. J.; Weix, D. J.; Hansen, E. C. Metal-Reductant-Free Electrochemical Nickel-Catalyzed Couplings of Aryl and Alkyl Bromides in Acetonitrile. *Org Process Res. Dev.* **2019**, *23*, (8), 1746–1751. https://doi.org/10.1021/acs.oprd.9b00232.

(40) Perkins, R. J.; Pedro, D. J.; Hansen, E. C. Electrochemical Nickel Catalysis for Sp^2-Sp^3 Cross-Electrophile Coupling Reactions of Unactivated Alkyl Halides. *Org. Lett.* **2017**, *19* (14), 3755–3758. https://doi.org/10.1021/acs.orglett.7b01598.

(41) Jiao, K. J.; Liu, D.; Ma, H. X.; Qiu, H.; Fang, P.; Mei, T. S. Nickel-Catalyzed Electrochemical Reductive Relay Cross-Coupling of Alkyl Halides to Aryl Halides. *Angew. Chemie - Int. Ed.* **2019**, n/a, n/a. https://doi.org/10.1002/anie.201912753.

(42) Walker, B. R.; Sevov, C. S. An Electrochemically-Promoted, Nickel-Catalyzed, Mizoroki-Heck Reaction. *ACS Catal.* **2019**, *9*, (8), 7197–7203. acscatal.9b02230. https://doi.org/10.1021/acscatal.9b02230.

(43) Manabe, S.; Wong, C. M.; Sevov, C. S. Direct and Scalable Electroreduction of Triphenylphosphine Oxide to Triphenylphosphine. *J. Am. Chem. Soc.* **2020**, *14*, jacs.9b12112. https://doi.org/10.1021/jacs.9b12112.

(44) Matsubara, K.; Yamamoto, H.; Miyazaki, S.; Inatomi, T.; Nonaka, K.; Koga, Y.; Yamada, Y.; Veiros, L. F.; Kirchner, K. Dinuclear Systems in the Efficient Nickel-Catalyzed Kumada–Tamao–Corriu Cross-Coupling of Aryl Halides. *Organometallics* **2016**, *36* (2), 255–265. https://doi.org/10.1021/acs.organomet.6b00451.

(45) Yamamoto, T.; Wakabayashi, S.; Osakada, K. Mechanism of C-C Coupling Reactions of Aromatic Halides, Promoted by Ni ($COD)_2$, in the Presence of 2,2'-bipyridine and PPh_3, to Give Biaryls. *J. Organomet. Chem.* **1992**, *428*, 223–237. https://doi.org/10.1016/0022-328X(92)83232-7

(46) Hansen, E. C.; Pedro, D. J.; Wotal, A. C.; Gower, N. J.; Nelson, J. D.; Caron, S.; Weix, D. J. New Ligands for Nickel Catalysis from Diverse Pharmaceutical Heterocycle Libraries. *Nat. Chem.* **2016**, *8* (12), 1126–1130. https://doi.org/10.1038/nchem.2587.

(47) Everson, D. A.; Buonomo, J. A.; Weix, D. J. Nickel-Catalyzed Cross-Electrophile Coupling of 2-Chloropyridines with Alkyl Bromides. *Synlett* **2014**, *25* (2), 233–238. https://doi.org/10.1055/s-0033-1340151.

(48) Siegl, W. O. Metal Ion Activation of Nitriles. Syntheses of 1,3-Bis(Arylimino)Isoindolines. *J. Org. Chem.* **1977**, *42* (11), 1872–1878. https://doi.org/10.1021/jo00431a011.

(49) Ciszewski, J. T.; Mikhaylov, D. Y.; Holin, K. V.; Kadirov, M. K.; Budnikova, Y. H.; Sinyashin, O.; Vicic, D. A. Redox Trends in Terpyridine Nickel Complexes. *Inorg. Chem.* **2011**, *50* (17), 8630–8635. https://doi.org/10.1021/ic201184x.

(50) Mohadjer Beromi, M.; Banerjee, G.; Brudvig, G. W.; Hazari, N.; Mercado, B. Q. Nickel(I) Aryl Species: Synthesis, Properties, and Catalytic Activity. *ACS Catal.* **2018**, *8* (3), 2526–2533. https://doi.org/10.1021/acscatal.8b00546.

(51) Onaka, M.; Matsuoka, Y.; Mukaiyama, T. A Convenient Method for the Direct Preparation of Ketones From 2-(6-(2-Methoxyethyl)pyridyl)carboxylates and Alkyl Iodides by Use of Zinc Dust and a Catalytic Amount of Nickel Dichloride. *Chem. Lett.* **1981**, *10* (4), 531–534. https://doi.org/10.1246/cl.1981.531.

(52) Amatore, C.; Jutand, A.; Périchon, J.; Rollin, Y. Mechanism of the Nickel-Catalyzed Electrosynthesis of Ketones by Heterocoupling of Acyl and Benzyl Halides. *Monatshefte fur Chemie* **2000**, *131* (12), 1293–1304. https://doi.org/10.1007/s007060070008.

(53) Biswas, S.; Weix, D. J. Mechanism and Selectivity in Nickel-Catalyzed Cross-Electrophile Coupling of Aryl Halides with Alkyl Halides. *J. Am. Chem. Soc.* **2013**, *135* (43), 16192–16197. https://doi.org/10.1021/ja407589e.

(54) Suga, T.; Ukaji, Y. Nickel-Catalyzed Cross-Electrophile Coupling between Benzyl Alcohols and Aryl Halides Assisted by Titanium Co-Reductant. *Org. Lett.* **2018**, *20* (24), 7846–7850. https://doi.org/10.1021/acs.orglett.8b03367.

(55) Wang, Z.; Li, X.; Sun, H.; Fuhr, O.; Fenske, D. Synthesis of NHC Pincer Hydrido Nickel Complexes and Their Catalytic Applications in Hydrodehalogenation. *Organometallics* **2018**, *37* (4), 539–544. https://doi.org/10.1021/acs.organomet.7b00848.

(56) Rettenmeier, C. A.; Wenz, J.; Wadepohl, H.; Gade, L. H. Activation of Aryl Halides by Nickel(I) Pincer Complexes: Reaction Pathways of Stoichiometric and Catalytic Dehalogenations. *Inorg. Chem.* **2016**, *55* (16), 8214–8224. https://doi.org/10.1021/acs.inorgchem.6b01448.

(57) Rettenmeier, C.; Wadepohl, H.; Gade, L. H. Stereoselective Hydrodehalogenation via a Radical-Based Mechanism Involving T-Shaped Chiral Nickel(I) Pincer Complexes. *Chem. - A Eur. J.* **2014**, *20* (31), 9657–9665. https://doi.org/10.1002/chem.201403243.

(58) Deng, Q.-H.; Wadepohl, H.; Gade, L. H. The Synthesis of a New Class of Chiral Pincer Ligands and Their Applications in Enantioselective Catalytic Fluorinations and the Nozaki–Hiyama–Kishi Reaction. *Chem. – A Eur. J.* **2011**, *17* (52), 14922–14928. https://doi.org/10.1002/chem.201102375.

(59) Khrizanforov, M.; Strekalova, S.; Khrizanforova, V.;

Grinenko, V.; Kholin, K.; Kadirov, M.; Burganov, T.; Gubaidullin, A.; Gryaznova, T.; Sinyashin, O.; Xu, L.; Vicic, D. A.; Budnikova, Y. Iron-Catalyzed Electrochemical C–H Perfluoroalkylation of Arenes. *Dalt. Trans.* **2015**, *44* (45), 19674–19681. https://doi.org/10.1039/C5DT03009A.

(60) Diccianni, J. B.; Diao, T. Mechanisms of Nickel-Catalyzed Cross-Coupling Reactions. *Trends Chem.* **2019**, *1* (9), 830–844. https://doi.org/10.1016/j.trechm.2019.08.004.

(61) Diccianni, J. B.; Katigbak, J.; Hu, C.; Diao, T. Mechanistic Characterization of (Xantphos)Ni(I)-Mediated Alkyl Bromide Activation: Oxidative Addition, Electron Transfer, or Halogen-Atom Abstraction. *J. Am. Chem. Soc.* **2019**, *141* (4), 1788–1796. https://doi.org/10.1021/jacs.8b13499.

(62) Jones, G. D.; Martin, J. L.; McFarland, C.; Allen, O. R.; Hall, R. E.; Haley, A. D.; Brandon, R. J.; Konovalova, T.; Desrochers, P. J.; Pulay, P.; Vicic, D. A. Ligand Redox Effects in the Synthesis, Electronic Structure, and Reactivity of an Alkyl−Alkyl Cross-Coupling Catalyst. *J. Am. Chem. Soc.* **2006**, *128* (40), 13175–13183. https://doi.org/10.1021/ja063334i.

(63) Sandford, C.; Fries, L. R.; Ball, T. E.; Minteer, S. D.; Sigman, M. S. Mechanistic Studies into the Oxidative Addition of Co(I) Complexes: Combining Electroanalytical Techniques with Parameterization. *J. Am. Chem. Soc.* **2019**, *141* (47), 18877–18889. https://doi.org/10.1021/jacs.9b10771.

(64) Gutierrez, O.; Tellis, J. C.; Primer, D. N.; Molander, G. A.; Kozlowski, M. C. Nickel-Catalyzed Cross-Coupling of Photoredox-Generated Radicals: Uncovering a General Manifold for Stereoconvergence in Nickel-Catalyzed Cross-Couplings. *J. Am. Chem. Soc.* **2015**, *137* (15), 4896–4899. https://doi.org/10.1021/ja513079r.

(65) Breitenfeld, J.; Wodrich, M. D.; Hu, X. Bimetallic Oxidative Addition in Nickel-Catalyzed Alkyl–Aryl Kumada Coupling Reactions. *Organometallics* **2014**, *33* (20), 5708–5715. https://doi.org/10.1021/om500506y.

(66) Chen, Z.; Qin, Y.; Amine, K. Redox Shuttles for Safer Lithium-Ion Batteries. *Electrochim. Acta* **2009**, *54* (24), 5605–5613. https://doi.org/http://dx.doi.org/10.1016/j.electacta.2009.05.017.

(67) Weng, W.; Huang, J.; Shkrob, I. A.; Zhang, L.; Zhang, Z. Redox Shuttles with Axisymmetric Scaffold for Overcharge Protection of Lithium-Ion Batteries. *Adv. Energy Mater.* **2016**, *6* (19). https://doi.org/10.1002/aenm.201600795.

(68) Chen, Z.; Liu, J.; Jansen, A. N.; GirishKumar, G.; Casteel, B.; Amine, K. Lithium Borate Cluster Salts as Redox Shuttles for Overcharge Protection of Lithium-Ion Cells. *Electrochem. Solid-State Lett.* **2010**, *13* (4), A39. https://doi.org/10.1149/1.3299251.

(69) Moshurchak, L. M.; Buhrmester, C.; Dahn, J. R. Triphenylamines as a Class of Redox Shuttle Molecules for the Overcharge Protection of Lithium-Ion Cells. *J. Electrochem. Soc.* **2008**, *155* (2), A129. https://doi.org/10.1149/1.2816229.

(70) Moshurchak, L. M.; Buhrmester, C.; Wang, R. L.; Dahn, J. R. Comparative Studies of Three Redox Shuttle Molecule Classes for Overcharge Protection of $LiFePO_4$-Based Li-Ion Cells. *Electrochim. Acta* **2007**, *52* (11), 3779–3784. https://doi.org/10.1016/j.electacta.2006.10.068.

(71) Kaur, A. P.; Ergun, S.; Elliott, C. F.; Odom, S. A. 3,7-Bis(Trifluoromethyl)-N-Ethylphenothiazine: A Redox Shuttle with Extensive Overcharge Protection in Lithium-Ion Batteries. *J. Mater. Chem. A* **2014**, *2* (43), 18190–18193. https://doi.org/10.1039/C4TA04463K.

(72) Kaur, A. P.; Casselman, M. D.; Elliott, C. F.; Parkin, S. R.; Risko, C.; Odom, S. A. Overcharge Protection of Lithium-Ion Batteries above 4 V with a Perfluorinated Phenothiazine Derivative. *J. Mater. Chem. A* **2016**, *4* (15), 5410–5414. https://doi.org/10.1039/C5TA10375D.

(73) Francke, R.; Little, R. D. Redox Catalysis in Organic Electrosynthesis: Basic Principles and Recent Developments. *Chem. Soc. Rev.* **2014**, *43* (8), 2492–2521. https://doi.org/10.1039/C3CS60464K.

(74) Peters, B. K.; Rodriguez, K. X.; Reisberg, S. H.; Beil, S. B.; Hickey, D. P.; Kawamata, Y.; Collins, M.; Starr, J.; Chen, L.; Udyavara, S.; Klunder, K.; Gorey, T. J.; Anderson, S. L.; Neurock, M.; Minteer, S. D.; Baran, P. S. Scalable and Safe Synthetic Organic Electroreduction Inspired by Li-Ion Battery Chemistry. *Science* **2019**, *363* (6429), 838–845. https://doi.org/10.1126/science.aav5606.

(75) Sevov, C. S.; Hickey, D. P.; Cook, M. E.; Robinson, S. G.; Barnett, S.; Minteer, S. D.; Sigman, M. S.; Sanford, M. S. Physical Organic Approach to Persistent, Cyclable, Low-Potential Electrolytes for Flow Battery Applications. *J. Am. Chem. Soc.* **2017**, *139* (8), 2924–2927. https://doi.org/10.1021/jacs.7b00147.

(76) Brushett, F. R.; Liao, C.; Kowalski, J. A.; Zhang, Z.; Shkrob, I. A.; Moore, J. S.; Huang, J.; Pan, B.; Vijayakumar, M.; Duan, W.; Wang, W.; Liu, J.; Zhang, L.; Yang, Z.; Milshtein, J. D.; Walter, E.; Li, B.; Wei, X. "Wine-Dark Sea" in an Organic Flow Battery: Storing Negative Charge in 2,1,3-Benzothiadiazole Radicals Leads to Improved Cyclability. *ACS Energy Lett.* **2017**, *2* (5), 1156–1161. https://doi.org/10.1021/acsenergylett.7b00261.

(77) Liu, Q.; Shinkle, A. A.; Li, Y.; Monroe, C. W.; Thompson, L. T.; Sleightholme, A. E. S. Non-Aqueous Chromium Acetylacetonate Electrolyte for Redox Flow Batteries. *Electrochem. commun.* **2010**, *12* (11), 1634–1637. https://doi.org/http://dx.doi.org/10.1016/j.elecom.2010.09.013.

(78) Sevov, C. S.; Brooner, R. E. M.; Chénard, E.; Assary, R. S.; Moore, J. S.; Rodríguez-López, J.; Sanford, M. S. Evolutionary Design of Low Molecular Weight Organic Anolyte Materials for Applications in Nonaqueous Redox Flow Batteries. *J. Am. Chem. Soc.* **2015**, *137* (45), 14465–14472. https://doi.org/10.1021/jacs.5b09572.

(79) Sevov, C. S.; Fisher, S. L.; Thompson, L. T.; Sanford, M. S. Mechanism-Based Development of a Low-Potential, Soluble, and Cyclable Multielectron Anolyte for Nonaqueous Redox Flow Batteries. *J. Am. Chem. Soc.* **2016**, *138* (47), 15378–15384. https://doi.org/10.1021/jacs.6b07638.

(80) Barel, Offir; Lidor-Hadas, Ramy; Gottesfeld, Ronen; Mizrahi, Orel, Yosef; Bergh, Anders, Olof Ingemar; Nguyen, B. V. Process for Preparing Pridopidine. WO2017015609 (A1), 2017.

(81) Yin, H.; Zhao, C.; You, H.; Lin, K.; Gong, H. Mild Ketone Formation via Ni-Catalyzed Reductive Coupling of Unactivated Alkyl Halides with Acid Anhydrides. *Chem. Commun.* **2012**, *48* (56), 7034. https://doi.org/10.1039/c2cc33232a.

(82) Hansen, E. C.; Li, C.; Yang, S.; Pedro, D.; Weix, D. J. Coupling of Challenging Heteroaryl Halides with Alkyl Halides via Nickel-Catalyzed Cross-Electrophile Coupling. *J. Org. Chem.* **2017**, *82* (14), 7085–7092. https://doi.org/10.1021/acs.joc.7b01334.

(83) Dudkina, Y. B.; Mikhaylov, D. Y.; Gryaznova, T. V.; Tufatullin, A. I.; Kataeva, O. N.; Vicic, D. A.; Budnikova, Y. H. Electrochemical Ortho Functionalization of 2-Phenylpyridine with Perfluorocarboxylic Acids Catalyzed by Palladium in Higher Oxidation States. *Organometallics* **2013**, *32* (17), 4785–4792. https://doi.org/10.1021/om400492g.

(84) Note: reported current densities are often the apparent current density based the submerged area of the electrode, rather than the active surface area as determined by electrochemical

measurements of capacitance. Here, the apparent current density is 15 mA/cm^2 (30 mA at a 1 cm x 1 cm piece electrode) and the current density based on electrochemically-measured area is 6.7 mA/cm^2.

Insert Table of Contents artwork here